Journal of Physics:
Conference Series

PAPER • OPEN ACCESS

Enhancing tribological performance of External Gear Pumps through CFD Analysis of Textured Surfaces and gear Edge Chamfering

To cite this article: Paolo Casoli *et al* 2024 *J. Phys.: Conf. Ser.* **2893** 012058

Enhancing tribological performance of External Gear Pumps through CFD Analysis of Textured Surfaces and gear Edge Chamfering

Paolo Casoli*[1], Hatami Garousi Masoud[1] and Carlo Maria Vescovini[1]

[1] Department of Engineering for Industrial Systems and Technologies, University of Parma, Italy

*E-mail: paolo.casoli@unipr.it

Abstract. External gear pumps (EGP) have become more and more common in a variety of industrial fields because of their advantageous cost-performance ratio, high efficiency, small design, and reliability. EGP are conceptually simple machines, but the design is often difficult, especially to ensure good performance at high working pressures. Among the internal components of EGP, the lateral plates are two important elements that strongly affect the performance of the machine. In this work, computational fluid dynamics (CFD) simulations are performed to investigate the effects of plate with textured surfaces and gear with chamfered edges on the bearing capacity. The simulations of the fluid flow in the oil gap between the gear tooth and the side bushing consider the correct pressure distribution at the inlet and outlet of the meatus, involving in the simulation also the portion of oil in the tooth space volumes surrounding the tooth.

1. Introduction

A gear pump is a mechanically simple device, but its small number of internal parts tend to interact with one another and significantly complicate the machine design, for this reason, having an accurate understanding of the machine is crucial to the design process.

This includes understanding of the lateral elements, gears, displacing action, motion transmission, and energy transfer, among other things [1,2]. The lateral plates are two crucial internal parts that have a significant impact on the machine operation. They are axial compensation plates designed to provide small gap heights with the gear wheels in order to reduce losses due to leakage. A lot of effort is put in improving bearing capacity between the gear wheels and the lateral plates, with the aim of preventing these two components from coming into direct contact with consequent excessive wear of the elements. Improving tribological performance of EGP could be achieved by optimizing the surface of side bushings and chamfering the edges of the gears. EGP can be designed with chamfered edges teeth and textured surfaces bushings for numerous reasons. Surface texturing on the lateral plates primarily help in increasing average pressures in the meatus that separates them form the gear wheels, amplifying hydrodynamic effects and increases bearing capacity. Edge chamfering on gear wheels is usually performed to decrease lateral plate material asportation caused by gear wheels themselves. To investigate the interaction of lateral plates texturing and gear wheels edges chamfering in EGP, a suitable mathematical model is developed in a multidimensional CFD environment. The CFD approach permits a detailed description of the lubricating gap [3]. Dahar and Vacca [4] introduced a novel Fluid Structure Interaction (FSI) model capable of predicting the lubricant film thickness in external gear machines (EGMs) under various operating conditions while accounting for elasto-hydrodynamic effects. The authors validated the model with experimental data to accurately simulate the behaviour of the lateral gaps and identifying the most suitable constraint method for lateral bushing deformation. A textured surface can significantly enhance hydrodynamic bearing capacity by increasing the average pressure between moving surfaces. Additionally, a lower friction coefficient can be achieved due to a reduced contact area and a larger average gap, which helps decrease overall surface wear. Yu et al. [5] conducted a numerical study on how the shape and orientation of dimples impact load capacity and friction coefficient, showing notable tribological improvements. Another benefit is the "hollow" effect, where dimples can store oil to prevent the failure of the lubricating film. To maximize the benefits of a textured surface, precise geometric design is crucial. This design process is challenging due to the many variables that can affect coupling performance. The characteristics of the dimples depend on the type of contact between the surfaces, operating conditions, and fluid properties [6].

Several researchers have explored the aforementioned solutions, Rahmani et al. [7] numerically analysed the effect of dimple distribution on load capacity and friction force in parallel thrust bearings, demonstrating significant improvements through surface geometry optimization. Etsion et al. [8] also reported excellent results using numerical models and experimental validation on parallel bearings. Additionally, other studies have examined surface texturing on circumferential seals. Both Kligerman et al. [9] and Razzaque et al. [10] showed that dimples generate a hydrodynamic force that reduces seal friction and wear. Gropper et al. [11] worked on the hydrodynamic lubrication of textured surfaces. They provide a comparative summary of different modeling techniques for fluid flow, cavitation, and micro-hydrodynamic effects for thrust bearing. Results showed that surface texturing remains a feasible method for contact performance enhancement in terms of load carrying capacity, minimum film thickness, friction, and wear. Casoli et al. [12,13] work on the performance improvements of EGP with helps of texturing surface and influence of its geometric characteristics on bearing capacity and frictional force. They used CFD simulations and bench tests to validate the efficiency of textured pumps; they have applied numerical analysis to a basic reference domain to examine the impact of the texture and the optimal dimple distribution for maximizing performance; the effect of cavitation between the dimples of the textured surface and cavitation effects on load capacity was investigated. In this paper, a 3D CFD model has been developed to analyse the bearing capacity in the lubrication gap inside an EGP, respect to previous papers [12, 13] the fluid in the tooth space volume at the two sides of the tooth has been considered in order to compute the effect of the fluid at the inlet and outlet of the meatus. This paper reports the challenge to define the boundary conditions for the surfaces defining the computational domain and to menage the domain interactions between the stationary and rotating parts. Once the best solutions to model and simulate the problem have been established, further investigations are carried out on the interaction of the tooth edge chamfer with the textured surface and its effects on the load-bearing capacity.

2. CFD model

An external gear pump from Casappa company with a displacement of 21.14 cm^3/rev has been selected for the analysis. The housing, lateral plates, driven gear, and driving gear are the three primary components of the pump.

The fluid in the tooth space volume and space between the lateral plates and the gear wheels in the low-pressure suction side, as shown in Fig. 1 (a), is the main subject of the investigation. The only part of the lateral plates where the texture has been added is the low-pressure section, suction side, which is also the most critical being the part with the minimum gap during pump operation. Simulation domain only considers a single tooth in suction side.

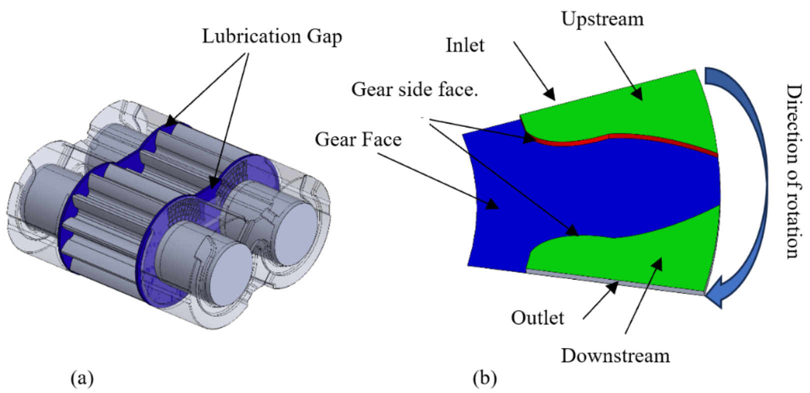

Figure 1. (a) Assembly of gear wheels and lateral plates. (b). Fluid domain regarding a single tooth with upstream and downstream space volumes. The name of the different surfaces that represents the boundaries of the fluid model are reported.

In Fig.1 (b) upstream and downstream tooth space volumes (highlighted green) are presented. If the gear is rotating in a clockwise direction, the fluid volume before the tooth is identified as upstream, and the fluid volume after the tooth as downstream. The numerical CFD study has been carried out with the code ANSYS© CFX.

The fluid modelled in the CFD simulations is an ISO VG-46 hydraulic oil, with a density of 850 kg/m^3 and dynamic viscosity of 46 mm^2/s at 40°C temperature.

In this first approach, the lateral plate is assumed to be parallel to the gear face. As in this simulation only one tooth is modelled with the fluid volume before and after the tooth itself, it is not possible to consider the gear as a combination of rotating walls, i

In fact, the gear flank walls (highlighted in red in Fig.1(b)) cannot be set as rotating walls in ANSYS CFX in steady-state simulations. In the previous study carried on by Casoli et al. [12, 13], where the gear flank walls were not part of the CFD model, the gear face parallel to the lateral plate could be thought of as a simple rotating wall, sliding with a velocity vector parallel to the wall itself, and the entire domain could be considered as a stationary domain. Fig. 2 shows the considered domain for simulation.

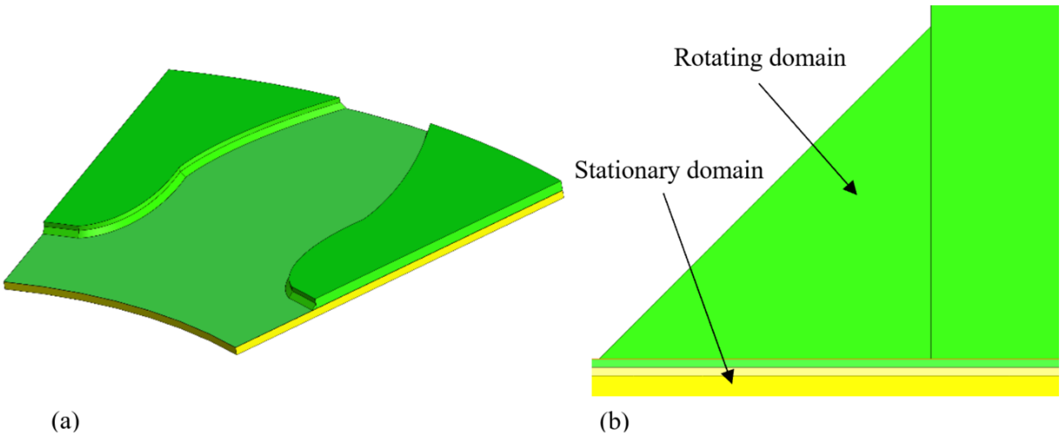

Figure 2. (a) flow domain. (b) stationary (yellow) and rotational (green) flow domain

To model the fluid volume presented in fig. 2(a), two different fluid domains, one stationary (yellow color) and one rotating domain (green color), have been identified, connected one to the other by means of a proper interface.

Aiming at producing meaningful results with CFD simulations, a fundamental aspect consists in defining the boundary conditions for the fluid domain based on the operating conditions of the EGP. Considering the single-tooth scenario on the suction side of the gear, there are alternatives for defining the domains boundary conditions based on pressure. It should be noticed that boundary conditions like mass flow rate or velocity-inlet and velocity-outlet could not be employed because there is no available information regarding the volume flow rate or velocity on this segment of the EGP. In previous study [13] all the boundary surfaces of the domain were considered as opening boundary, so in that case the flow could freely enter or exit the domain. In this study, many different surface boundary settings have been tested to find the best solution to obtain meaningful results, especially pressure and force in the lubrication gap.

In the subsequent lines the authors refer to the boundary surfaces reported and named in fig. 1 (b), in the following text, said surfaces are reported with italic font and capital letter.

Initially, the pressure-inlet for the *Inlet* surface boundary and pressure-outlet for the *Outlet* surface boundary have been evaluated, while *Upstream* and *Downstrea*m surfaces were treated as openings. However, in this case, a great deal of reverse flow in both *Inlet* and *Outlet* borders occurs, and the results show that there are high pressure tension regions at both the Inlet and the Outlet boundaries.

The next set of boundary conditions to be examined included symmetric boundary conditions for the *Upstream* and *Downstream* surfaces, as well as opening boundaries for the *Inlet* and *Outlet* surfaces. In this case, there are problems with velocity gradient at *Upstream* and *Downstream* boundaries because of the small thickness of the modelled domain. The velocity along the thickness of the vane space is not constant, and even a small change in the domain height will cause the velocity to change significantly. The symmetry boundary for *Upstream* and *Downstream* surfaces would be the best hypothesis, but only on condition that half of the domain height is modelled, which in this case would mean having a tooth space volume with a thickness of 16 mm, but the the number of the cells of the mesh would become very high.

Another alternative that has been taken into consideration was to employ the periodic boundary condition for the *Inlet* and *Outlet* surfaces and an opening boundary condition for the *Downstream* and *Upstream* surfaces. When two boundaries are regarded as periodic boundary conditions, flow can exit from one and simultaneously enter the other boundary. In this scenario, all velocity and pressure contours near the inlet and outlet result extremely smooth.

After extensive testing of various boundary condition scenarios, the solution rated as the best one was the one consisting in setting an opening boundary with a relative pressure of 1 bar for the *Upstream*, *Downstream*, *Inlet*, and *Outlet* surfaces.

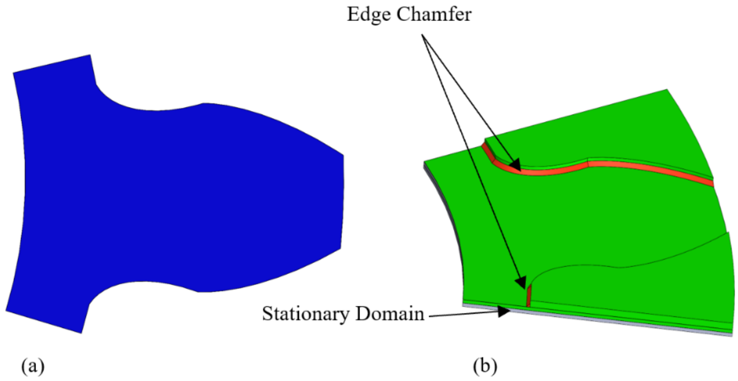

Figure 3. (a) Fluid domain considering only the meatus between gear tooth and lateral plate. (b) Fluid domain considering the meatus and the space volume at the sides of the gear tooth. The subdivision of this domain in rotating and stationary domain have been highlighted.

Different simulations have been carried on taking in considerations multiple factors. Two different sizes are considered for the tooth edge chamfer, being 0.1mm and 0.05 mm. In Fig.3 (b) edge chamfer faces are highlighted in red in the fluid domain. Regarding the lubrication gap, two distinct thicknesses of 5 μm and 10 μm are simulated. The considered portion of the vanes at the sides of the tooth has a height of 0.2 mm. This height has been found to be sufficient to guarantee good results while being small enough to keep the number of elements and therefore simulations time in an acceptable range. The simulations have been run for two different pump rotational speeds, being 2500 rev/min and 5000 rev/min. The latter of the two rotational speeds may seem out of range for this kind of pump but this value finds his own reason. The trend in industry is in fact to bring these kinds of machines to increased rotational speeds to follow the electrification process which requires pump performances higher than before.

During the preliminary phase, when testing the different boundary conditions sets in order to define which one to use, the texture surface was not taken into consideration to maintain the model as simple as possible and speed up the test phase.

The domain has been meshed using structured mesh, with the aim of having a good control on the elements disposition and characteristics all over the fluid domain. A mesh sensitivity process has also been performed. Three distinct meshes have been produced for the domain meshing process by varying the boundary layers grid size. In the final mesh (Mesh3), there were roughly 1’300’000 cells, compared to the initial basic mesh 750’000 cells. The parameter used to evaluate the influence of the mesh on the numerical results is the force generated by the pressure on the gear face, that is the surface integral of local pressure in gear surface area. The results for the three cases, expressed as a ratio of the maxim value for confidential reasons, are shown in Fig. 4.

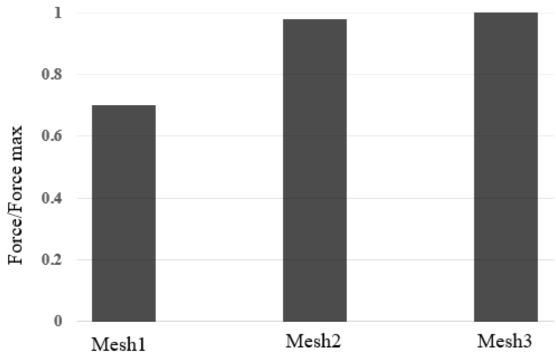

Figure 4. Mesh sensitivity charts.

The diagram shows that the difference visible between the first two meshes is significant and decreases with subsequent cases. The maximum pressure value stabilizes from the Mesh 3, indicating that further mesh refinement only slightly affects the results. For this reason, the Mesh 2 model has been chosen for further simulation studies that were carried out.

Pressure distribution on the gear face for 5-micron gap thickness with and without chamfer is shown in Fig.5

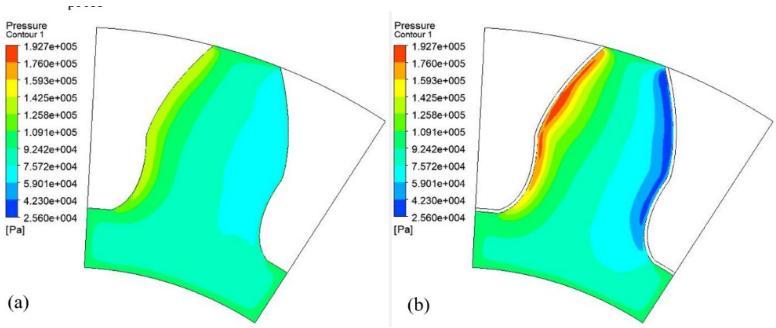

Figure 5. Absolute Pressure distribution on gear face for 5 microns gap.
(a) Without chamfer. (b) With chamfer.

In Fig. 5 rotational direction of gear is counterclockwise. It is clear that by adding the chamfer the pressure distribution in the gap presents higher peak values, both negative and positive. In this case calculated pressure distribution in the balanced tooth and this contour provide a strong indication that balanced tooth is influenced by chamfer. Results for two different lubrication gaps shows that by decreasing the lubrication gap thickness, pressure increases and adding chamfer to domain increases the maximum pressure.

Next step is to consider the texturing surface. Simulations have been carried out with and without the presence of the chamfer edge. A configuration known as partial texturing is the ideal geometric arrangement of the dimples within the domain to enhance the bearing capacity, according to previous studies [12,13]. Only a small percentage of the entire domain has dimples, and the optimal situation occurs when 45–60% of the domain is textured. The optimum texture is shown in Fig.6.

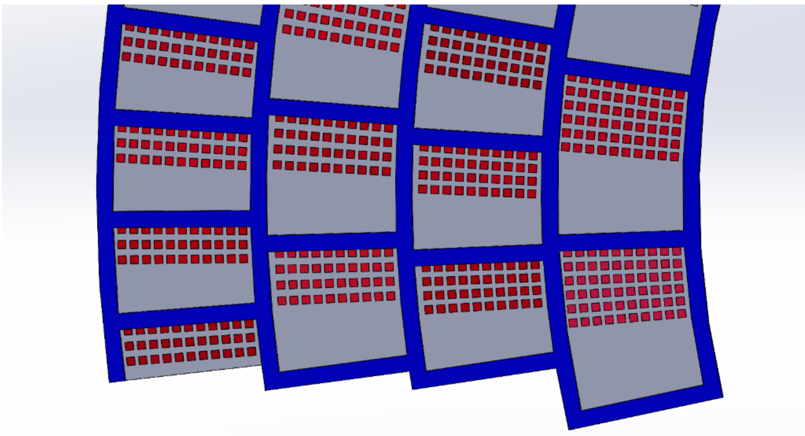

Figure 6. Texturing surface on the bushing suction side.

In Fig. 6 dimples are highlighted in red, while the channels, with greater depth, are in blue; this channel has an essential role: it permits to restore the pressure conditions at the inlet and outlet of each portion of the domain [12, 13]. A sensitivity analysis has been used to determine the properties of the structured mesh that has been used to discretize the fluid domain. The convergence of the solution was judged by examining the residual levels and additional quantities such as the mass flow rate balances. The convergence criterion for the analysis has been reduced from the default value of 1×10^{-3} for residual to 1×10^{-5}.

Based on the results from [13] there are not significant differences in reaction forces for different positions of the gear tooth respect to the textured surface realized in the bushing. For this reason, in this study simulations are performed considering a single tooth position respect to the texturing.

Fig. 7 shows the pressure distribution for texturing surface with and without up and down stream in 10 micron lubrication gap thicknesses. In this case there is no chamfer on the edge of the gear tooth.

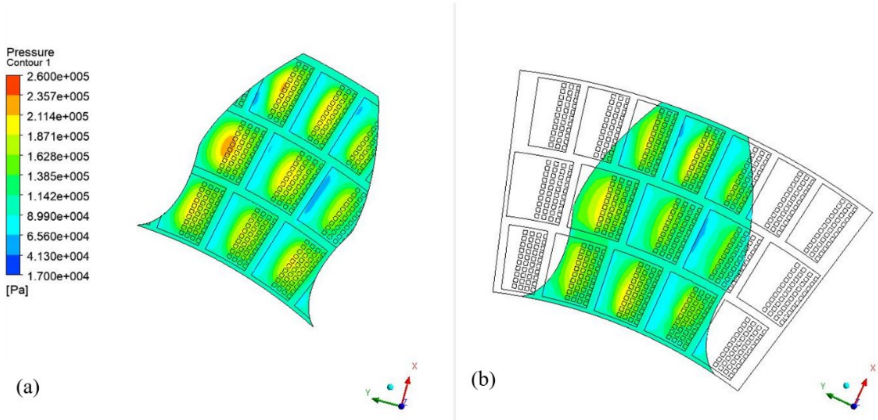

Figure 7. Pressure contour in gap 10µm and 2500rpm. (a) without up and down stream. (b) with up and down stream

In Fig. 7 the rotational direction of the moving plane is counterclockwise. By observing the pressure contours, an overpressure is established in each sector of the textued surface proving the capability of texturing of generating a positive bearing capacity. Since the speed of the moving plane is rotational, the sliding velocity rises as the radius increases, leading to a growth in the hydrodynamic effect that allows to generate a greater overpressure in correspondence with the sectors at a greater distance from the center of rotation. A slight decrease in pressure values in the dimples regions can be seen when considering the up and down stream volumes in the simulation: the side opening surfaces are far from the gear walls, so pressure in this case will decrease. Due to decrease in pressure, bearing capacity also decreases. Fig. 8 shows the force generated by the gear surface. For confidentiality reasons, the bearing capacity was normalized with respect to the maximum value.

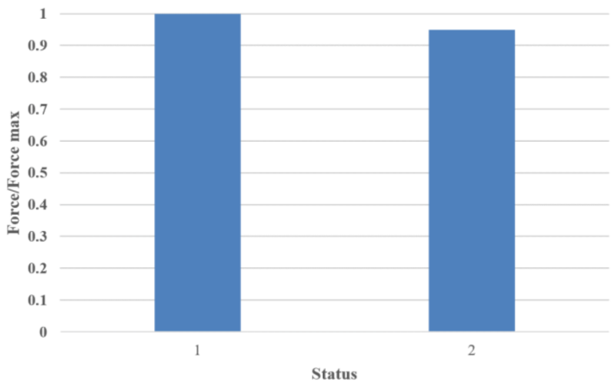

Figure 8. Bearing capacity without (1) and with (2) considering up and down streams.

In Fig. 8, status 1 refers to the case in which the domain is limited to the meatus between the gear tooth and the lateral plate while status 2 refers to the case in which the domain with up and down stream regions are considered. By considering the up and down stream regions, in this case without chamfer edge, there are no relevant differences in hydrodynamic pressure.

To investigate the effects of the tooth edge chamfering, some simplification have to be made: the hypotesis of a fixed and uniform gap height and the uniform and constant pressure in boundaries permit to focus on the differences between a case with and without a chamfer. As it was said before, edge chamferings of 0.1 mm and 0.05 mm for have been considered. Fig. 8 shows the pressure distribution between the tooth gear and the lateral plate textured surface with and without the 0.1 mm chamfering for 5 μm thick gap.

Journal of Physics: Conference Series **2893** (2024) 012058 doi:10.1088/1742-6596/2893/1/012058

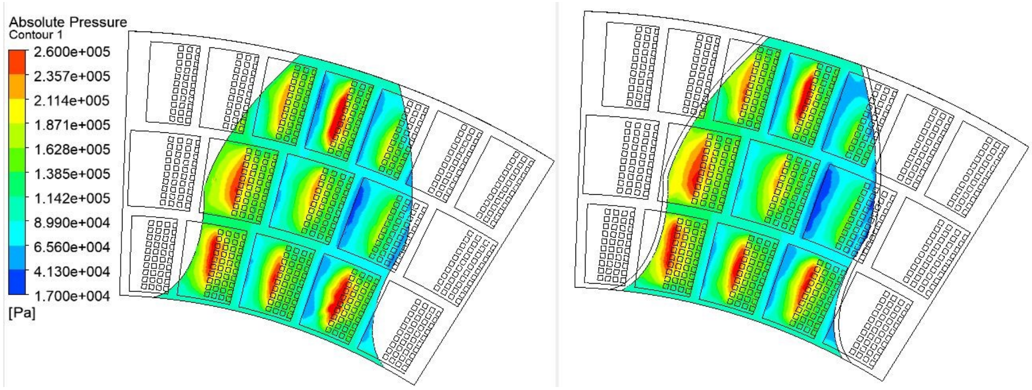

(a) (b)

Figure 9. Pressure contour in gap 5μm and 2500rpm. (a) Without chamfer (b) With chamfer 0.1mm

As it can be seen in Fig. 9, in the case of chamfered tooth edge, maximum pressure regions present slightly lower pressure values, while the low-pressure regions look slightly wider. According to the results reported in Fig. 9, the differences between the two cases, with and without a chamfer, is very small, but it's still interesting that the case with chamfer tends to generate a lower maximum pressure if compared to the one without chamfer.

Pressure distribution for chamfer of 0.1 mm and 0.05 mm for 10 μm lubrication gap are shown in fig. 10.

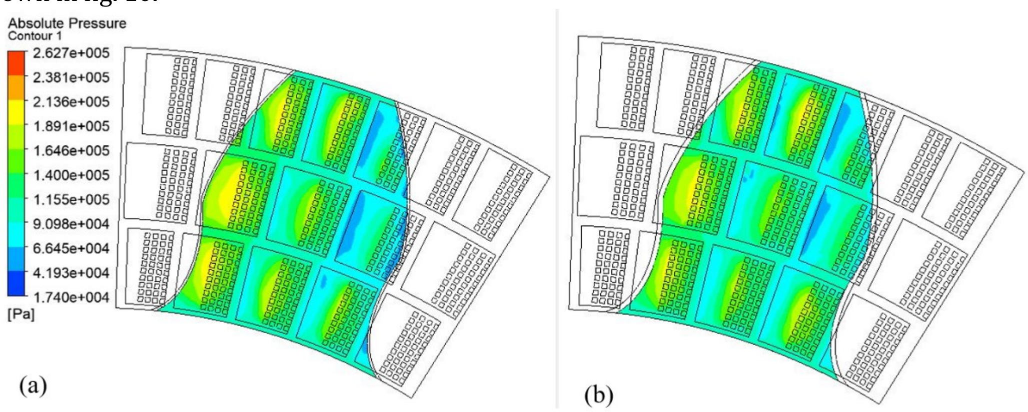

Figure 10. Pressure contour in gap 10μm and 2500rpm. (a) Chamfer 0.05mm. (b) Chamfer 0.1mm

In Fig. 10 it is possible to notice little differences in the pressure contours of the reported cases of the gear tooth with 0.05 mm chamfer and the one with 0.1 mm chamfer. The comparison shows that by increasing the size of the chamfer, the maximum pressure and the extent of regions with high pressure both decrease. The bar graph in Fig. 11 shows the force generated on the gear face with different sizes of the chamfer, included the case of edge without any chamfering. Datas for gap thicknesses of 5 μm and 10 μm and for a pump speed of 2500 rev/min are reported. For reasons of confidentiality the bearing capacity has been divided by the maximum value obtained.

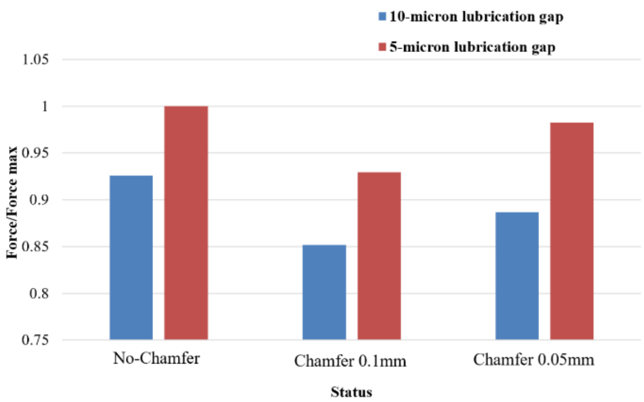

Figure 11. Bearing capacity in two different chamfer size with and without chamfer - 2500 rpm

As it is possible to see, the decrease of pressure values noticed in the pressure contours have an obvious effect on the bering capacity on the gear tooth: by increasing the size of the chamfer, bearing capacity decreases for both the cases of 10 μm and 5 μm gap thickness.

In the next step, effects of rotational speed on the pressure distribution and bearing capacity has been inspected. Two different rotational speed of 2500 rpm and 5000 rpm has been took into consideration. Pressure distribution for 10 μm gap in 5000 rpm is shown in Fig.12.

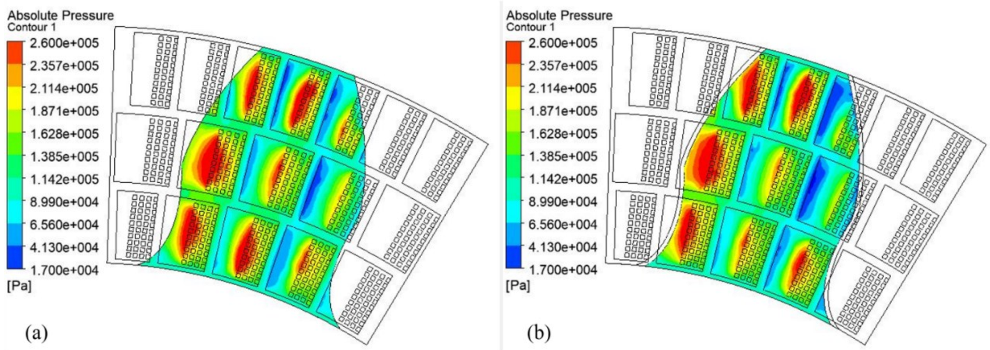

Figure 12. Pressure contour in gap 10μm and 5000rpm. (a) without chamfer. (b) with Chamfer 0.1mm

As can be seen in Fig.12, by increasing the rotational speed, pressure in the dimples regions increases. Low-pressure near the channels for the chamfering case increases and high pressure regions in the chamfered edge case decrease if compared to the case without chamfer. Having a chamfer on the tooth edge, the flow has an easier access to the gap between the gear face and lateral bushing and because of that the pressure contour near the tooth edge looks smoother for the chamfer edge case.

Fig.13 shows the force generated by the gear face for 10 μm and 5 μm gaps, with and without chamfering effects. Similarly to the case at lower speed, applying a chanfer to the tooth edge leads to a slighlty reduced bearing capacity. By the way, effects of force decreasing due to chamfer is lower than in the low-rotational speed conditions.

For reasons of confidentiality the bearing capacity has been divided by the maximum value obtained.

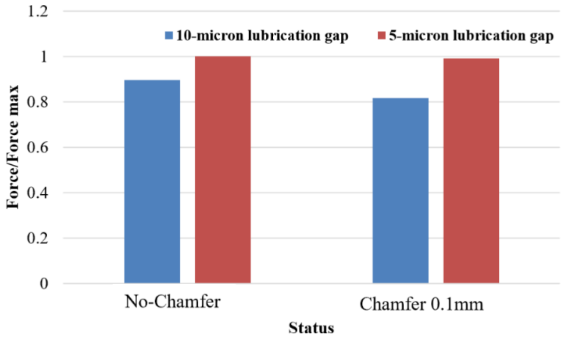

Figure 13. Bearing capacity with and without considering chamfer effects in 10 and 5 μm lubrication gap thickness at 5000rpm rotational speed.

3. Conclusion

In this work a CFD model has been developed with the aim of analysing the bearing capacity in the lubrication gaps of EGP. Different scenarios for boundary conditions have been studied and best scenario introduced.

Effects of considering the flow domain before and after the tooth and effects of chamfer in the pressure distribution have been studied, and results show that in absence of texturing surface, applying a chamfer to the tooth edge increases the negative and positive peak pressuers on the gear face. Starting from the work published on previous papers, textured surface study has been performed considering a more complete domain and the effects of edge chamfer, inspecting the effects on the bearing capacity in two different lubrication gap thickness with two different chamfer size of 0.1 mm and 0.05mm. The results show that by applyng a chamfer to the tooth edge leads to a slight decrease in the maximum pressure between the gear tooth and the textured lateral plate with a consequent in the bearing capacity. Finally, the effects of rotational speed on gear pressure distribution and bearing capacity has been studied, and results showed that increasing the rotational speed causes an increase the pressure generated in the lubrication gap. Also at high speed, the application of a chamfer leads to a reduction in pressure values and therefore in bearing capacity. By the way, in each one of the cases considered and simulated, the reduction in pressure values and bearing capacity is not significant which suggest that edge chamfering is a practise which doesn't produce important performance reduction for textured lateral plates pumps.

Acknowledgement

The authors would like to acknowledge the active support of this research by Casappa S.p.A., Parma, Italy.

References

[1] Vacca, A., Dhar, S., & Opperwall, T. (2011, May). A coupled lumped parameter and CFD approach for modeling external gear machines. In SICFP2011 The Twelfth Scandinavian International Conference on Fluid Power.

[2] Zecchi, M., Vacca, A., & Casoli, P. (2010). Numerical analysis of the lubricating gap between bushes and gears in external spur gear machines. Fluid P, 397.

[3] Casoli, P., Vacca, A., & Berta, G. L. (2006). A numerical model for the simulation of flow in hydraulic external gear machines. In Power Transmission and Motion Control (Vol. 1, pp. 147-168). BATH.
[4] Dhar, S., & Vacca, A. (2013). A fluid structure interaction—EHD model of the lubricating gaps in external gear machines: Formulation and validation. Tribology International, 62, 78-90.
[5] Yu H, Wang X, Zhou F, Geometric Shape Effects of Surface Texture on the Generation of Hydrodynamic Pressure Between Conformal Contacting Surfaces, Tribology Letters, 2010, Volume 37, Issue 2, pp 123–130. DOI: https://doi.org/10.1007/s11249-009-9497-4
[6] Dobrica M B, Fillon M, Pascovici M D, Cicone T, Optimizing surface texture for hydrodynamic lubricated contacts using a mass-conserving numerical approach, Proceedings of the Institution of Mechanical Engineers Part J Journal of Engineering Tribology, 2010, Volume: 224 issues: 8, pp 737–750
[7] Rahmani R, Shirvani A, Shirvani H, Optimization of Partially Textured Parallel Thrust Bearings with Square-Shaped Micro-Dimples, Tribology transactions, 2007, 50:3, 401-406, DOI: 10.1080/10402000701429261
[8] Etsion I, Halperin G, Brizmer V, Klingerman Y, Experimental investigation of laser surface textured parallel thrust bearings, Tribology Letters, 2003, Volume 17, pp 295–300
[9] Kligerman Y, Etsion I, Analysis of the Hydrodynamic Effects in a Surface Textured Circumferential Gas Seal, Tribology Transactions, 2001, Volume 44, Issue 3, pp 472–478
[10] Razzaque M M, Faisal T R, Performance of Mechanical Face Seals with Surface Micropores, Journal of Mechanical Engineering, 2008, Volume 37, pp 77–80
[11] Gropper, D., Wang, L., & Harvey, T. J. (2016). Hydrodynamic lubrication of textured surfaces: A review of modeling techniques and key findings. Tribology international, 94, 509-529.
[12] Casoli P., Scolari F., Rossi C., Rigosi M., A CFD design of engineered surface for tribological performance improvements in hydraulic pumps, (2020) 12th International Fluid Power Conference (12. IFK). Dresden, October 12 – 14, 2020. Volume 1 – Symposium. Dresden: Technische Universität Dresden, 2020. S. 341-349 (DOI: 10.25368/2020.6). DOI: 10.25368/2020.41
[13] Casoli, P.; Scolari, F.; Rundo, M.; Lettini, A.; Rigosi, M. CFD Analyses of Textured Surfaces for Tribological Improvements in Hydraulic Pumps.(2020) Energies,13 (21), DOI: 10.3390/en13215799